Structure and Morphology Changes in Absorbable Poly(glycolide) and Poly(glycolide-*co*-lactide) during in Vitro Degradation

Xin-Hua Zong, Zhi-Gang Wang, Benjamin S. Hsiao,* and Benjamin Chu

Department of Chemistry, State University of New York at Stony Brook, Stony Brook, New York 11794-3400

Jack J. Zhou, Dennis D. Jamiolkowski, Eugene Muse, and Edward Dormier

Ethicon, Inc., A Johnson & Johnson Company, Somerville, New Jersey 08876-0151

Received April 23, 1999

ABSTRACT: The changes of crystal structure and morphology in poly(glycolide), PGA, homopolymer and poly(glycolide-*co*-L-lactide), PGA-*co*-PLA, (90/10) random copolymer during in vitro degradation were investigated by gel permeation chromatography (GPC), wide-angle X-ray diffraction (WAXD), and small-angle X-ray scattering (SAXS). GPC results showed that the molecular weight and polydispersity decreased significantly during the first 2 weeks of degradation. In contrast, the mass degree of crystallinity, ϕ_{mc}, determined from WAXD showed an Avrami-like behavior in both polymers, increasing rapidly within the first 2 weeks and gradually reaching a plateau value. The effect of degradation on the crystal unit cell dimensions was noticeable and anisotropic, which may reflect the process of crystal perfection in vitro. Corresponding SAXS results also showed that the long period (L), lamellar thickness (l_c), and amorphous layer thickness (l_a) from the crystal lamellar stacks all decreased appreciably in both PGA and PGA-*co*-PLA samples during the first 3 weeks of degradation. By comparing molecular weight and lamellar thickness results, we conclude that the fully degraded chain fragments have an average length of about 3 times the crystal thickness. On the basis of these results, we propose that degradation proceeds through the combined processes of chain scission and cleavage-induced crystallization in the amorphous regions via two pathways. (1) The degradation occurs in the amorphous gaps between the crystal lamellar stacks, where the amorphous chains are broken leading to greater mobility to form new crystal lamellar stacks with thinner thickness. This process significantly reduces the averaged values of L, l_c, and l_a. (2) The degradation process also occurs in the amorphous layer domain between the adjacent lamellae within the lamellar stacks, where chain scission causes the rapid decrease in polydispersity.

Introduction

Among the many kinds of biodegradable polymers reported, the system of linear aliphatic polyesters is one of the few that can possess very high molecular weight (thus good melt processability and mechanical strength) and excellent degradation properties because of its extremely hydrolyzable backbones. Polyglycolide (PGA), polylactide (PLA), and its random copolymer poly(glycolide-*co*-lactide) (PGA-*co*-PLA) are typical examples of aliphatic polyesters, which are of good properties for biomedical applications mainly in degradable and absorbable sutures, implants, artificial skin grafts, and drug release systems.[1−3] The great advantage of these synthetic biocompatible and absorbable materials is that their degradability is due to simple hydrolysis of the ester backbone in aqueous environments such as the body fluids. Furthermore, the degradation products are ultimately metabolized to carbon dioxide and water or are excreted via the kidney.[4] The preferred method for producing high molecular weight PGA, PLA, and PGA-*co*-PLA (co)polymers is the ring-opening polymerization of the cyclic diesters of glycolide and lactide using antimony, zinc, lead, or tin catalysts, which has been discussed in detail before.[5]

The mechanism of degradation behavior in PGA, PLA, and PGA-*co*-PLA (co)polymers in the aqueous media has been widely investigated as functions of time, temperature, crystallinity, and the pH level on properties such as molecular weight and mechanical strength.[6−16] For example, Chu et al. have studied the effect of buffer solution on the degradation of PGA sutures and concluded the importance of crystallinity on the tensile strength.[10,11] They proposed that the degradation proceeds through two separate stages with different degradation rates, which correlates well with the amorphous and crystalline regions in the samples, respectively. Fredericks et al. have shown that hydrolytic attack of oriented fiber based on the copolymer of the present study is initiated in the amorphous areas.[12] As these materials are crystallizable, it is expected that morphological variables at the lamellae level during in vitro degradation must also be an important factor to affect the degradation mechanism.[17] In this paper, we have followed the changes of crystal and morphological parameters (2−100 nm) during in vitro degradation of unoriented plates of PGA homopolymer and PGA-*co*-PLA copolymer using wide-angle X-ray diffraction (WAXD) and small-angle X-ray scattering (SAXS) techniques. The degree of crystallinity and unit cell parameters (a, b, and c) were obtained from WAXD, and the lamellar morphological variables such as long period, lamellar thickness, and amorphous layer thickness were determined by the SAXS analysis. The corresponding changes of molecular weight and polydispersity were measured by gel permeation chromatography (GPC). The weight loss experiments were also carried out for comparison purposes. Some new insights into the degradation mechanism of PGA homopolymer and PGA-

* To whom correspondence should be addressed. E-mail bhsiao@notes.cc.sunysb.edu.

10.1021/ma990630p CCC: $18.00
Published on Web 11/11/1999

Table 1. GPC Results for Crystalline and Amorphous PGA and PGA-*co*-PLA (90/10) Samples during in Vitro Degradation

		time (weeks)							
		0	1	2	3	4	5	6	7
PGA (crystalline)	M_w	60000	18200	3000	2600	2354	2288	2218	2413
	M_n	23000	9400	2400	2200	2089	2048	1992	2100
	M_w/M_n	2.58	1.94	1.21	1.15	1.13	1.12	1.11	1.13
PGA (amorphous)	M_w	66000	3900						
	M_n	24000	2900						
	M_w/M_n	2.72	1.34						
PGA-*co*-PLA (90/10) (crystalline)	M_w	77000	31900	5200	3800	3054	2842	2734	2662
	M_n	24000	14300	3700	3000	2571	2447	2377	2333
	M_w/M_n	3.20	2.23	1.40	1.27	1.19	1.16	1.15	1.14
PGA-*co*-PLA (90/10) (amorphous)	M_w	73000	7000	2018	1963				
	M_n	24000	4600	1843	1794				
	M_w/M_n	2.97	1.53	1.09	1.09				

co-PLA copolymer have been obtained on the basis of these results.

Experimental Section

PGA homopolymer and PGA-*co*-PLA random copolymer were experimental materials supplied by Ethicon Inc. The melting temperatures of PGA and PGA-*co*-PLA were 220 and 201 °C, respectively, as measured by DSC at a heating rate of 20 °C/min. The PGA-*co*-PLA copolymer contained 90% glycolide acid and 10% L-lactide acid, with an inherent viscosity of 1.60 dL/g (as measured at 0.1 g/dL at 25 °C in hexafluoro-2-propanol). The nature of the randomness in the copolymer has been verified by the technique of NMR spectroscopy. The initial number-average and weight-average molecular weight (M_n and M_w) and polydispersity (M_w/M_n) of these samples can be found in Table 1.

Plates of PGA and PGA-*co*-PLA were produced by compression molding of raw pellets at 350 and 270 °C, respectively, using a pressure of 1.03×10^8 Pa for 3 s. The samples were made either amorphous by water quenching at room temperature or semicrystalline (termed crystalline from now on) by annealing at 110 °C for 24 h. (We did not observe any annealing or processing induced degradation in the samples, as seen in the molecular weight information in Table 1.) The molded plates were then cut into parallelepiped specimens ($15 \times 10 \times 2$ mm^3). (Despite the large dimension used, we did not observe any surface−core differentiation with lower molecular weight species in the core during degradation.) In vitro phosphate buffer solution (PBS) was prepared by dissolving 4.54 g of potassium phosphate (KH_2PO_4) and 14.2 g of sodium phosphate (Na_2HPO_4) into 2 L of distilled water. The pH value of PBS was 7.27 ± 0.06. All the specimens, either in amorphous or crystalline states, were weighed and placed into bottles, which were filled with PBS and tightly covered and incubated in vitro at temperature 37.0 ± 0.1 °C for desired time periods. These temperature and pH parameters were selected to simulate homeostasis conditions of the human body. At the end of each degradation period, the specimens were recovered, gently washed three times in distilled water, and dried in a vacuum oven at room temperature for 48 h, prior to the measurement.

The molecular weights (M_w and M_n) and polydispersity (M_w/M_n) of the samples were determined by GPC in hexafluoro-2-propanol (HFIP) at ambient temperature, using the Waters 410 apparatus with differential refractometer detector. The calibration was carried out using poly(methyl methacrylate) (PMMA) standards with narrow molecular weight distribution (MWD) (American Polymer Standards Corp.). The chromatographic data were sampled with Water 717 Plus autosampler, and the calculations were done with Waters Expertease chromatography software.

Wide-angle X-ray diffraction (WAXD) patterns of the samples were obtained using a Siemens Hi-Star X-ray area detector with Cu Kα radiation of wavelength 1.542 Å. The distance from sample to detector was 60 mm. The angular range of 2θ was 3−40°. From the WAXD data, the integrated intensities, peak positions, peak heights, and peak widths for crystal reflections and amorphous background were calculated by a deconvolution method (all peaks were chosen to be Gaussian) using the program GRAMS/32 Spectral Notebase (Galactic Industries Corp.). In this study, two Gaussian peaks were used to describe the amorphous background. By dividing the total intensities of the crystalline reflections I_c to the overall intensity I_{total}, a measure of the mass fraction of the crystalline phase in the sample can be obtained. This value is termed as the apparent mass degree of crystallinity, ϕ_{mc}. Because of possible distortions in the crystal lattice and thermal disorder, the measured value of I_c may be lower than the true value of crystallinity. The mass crystallinity is related to the volume degree of crystallinity, ϕ_{vc}, as $\phi_{mc} = f(T)\phi_{vc}$, where $f(T)$ is a temperature-dependent factor taking into account of the deviations mentioned above and the correction for translating the mass to the volume. The positions of the crystal reflection peaks were used to calculate the unit cell parameters.

Small-angle X-ray scattering (SAXS) patterns were obtained at the Advanced Polymers Beamline (X27C) in the National Synchrotron Light Source (NSLS), Brookhaven National Laboratory (BNL). The sample-to-detector distance used was 1746 mm. The wavelength was 1.307 Å. The SAXS patterns were recorded by means of a 2D imaging plate detector. The one-dimensional SAXS profile extracted from the 2D scattering pattern was analyzed via the method of correlation function for crystalline polymers. The theory of this approach can be found in previous papers.[18−21] With this method (after determining the Porod parameters, correcting the liquid scattering, and finite interface between the scattering phases), assuming that the system follows a two-phase lamellar stacks model, we can calculate several morphological variables including long period L, lamellar thickness l_c, and amorphous layer thickness l_a.[19]

Results and Discussion

Molecular Weight and Polydispersity during Degradation. The molecular weight information (M_w, M_n, and polydispersity (M_w/M_n)) measured by GPC is listed in Table 1. For better illustration of their changes during degradation, the data are also plotted in the following figures. Figures 1 and 2 show the changes of M_w, M_n, and M_w/M_n for PGA homopolymer and PGA-*co*-PLA copolymer occurring during the degradation period of 7 weeks, respectively. For both PGA and PGA-*co*-PLA samples, it is seen that degradation of the amorphous specimens is much faster than the crystalline ones. In fact, the amorphous PGA sample was degraded so fast that the sample could not be recovered from PBS after the first week. In contrast, for the amorphous PGA-*co*-PLA sample, molecular weight measurements could still be made until the third week. Under the in vitro conditions, it takes about 2 weeks to decrease the molecular weights (M_w) from 60 000 to 3000 and from 77 000 to 5200 for crystalline PGA and PGA-*co*-PLA samples, respectively. After this period, the

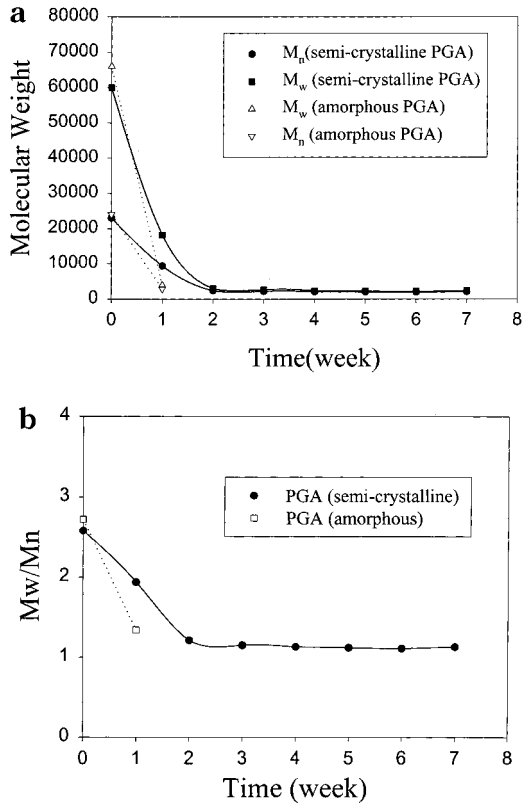

Figure 1. Changes of (a) molecular weight and (b) polydispersity for the crystalline and amorphous PGA samples during in vitro degradation.

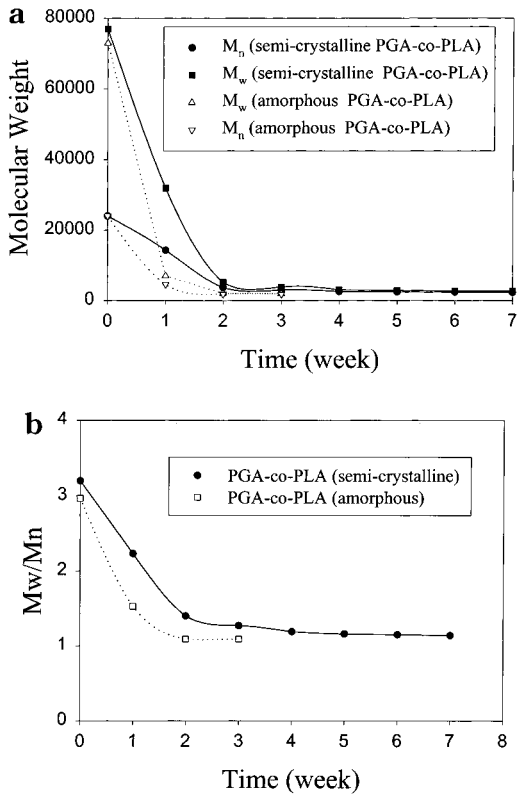

Figure 2. Changes of (a) molecular weight and (b) polydispersity for the crystalline and amorphous PGA-*co*-PLA (90/10) samples during in vitro degradation.

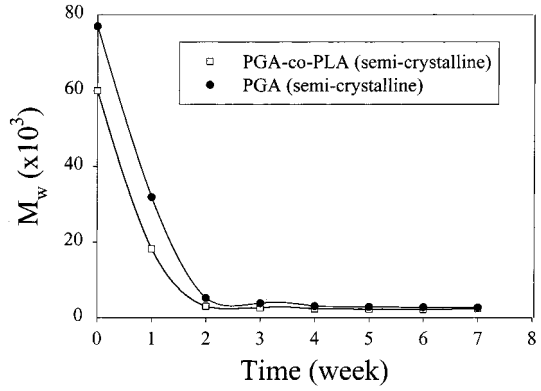

Figure 3. Changes of weight-averaged molecular weight (M_w) for crystalline PGA and PGA-*co*-PLA during in vitro degradation.

molecular weight decreases only very slightly, indicating that the residual amorphous materials are filled with small crystallites and the subsequent degradation becomes more difficult in the later period. The difference between the amorphous and crystalline samples also confirms that degradation is easier to take place in the amorphous regions than the crystalline regions. Significant decreases in polydispersity (from 2.58 to 1.15 for PGA and from 3.20 to 1.27) within 3 weeks (see Figures 1b and 2b) suggest that degradation happens not only in the amorphous pockets between the crystal lamellar stacks but also in the amorphous layers between the adjacent lamellae within the stacks, which will be discussed in detail later. The narrow value of polydispersity (near the unity) indicates that the degraded chain fragments have a similar length distribution. Figure 3 compares the degradation rates of crystalline PGA and PGA-*co*-PLA samples. It is seen that during the first 2 weeks their degradation rates are very similar.

It is well-known that the amorphous polyester samples have characteristically disordered chains, and the water molecules can easily diffuse into them, leading to rapid degradation through chain scission. While the crystalline samples also have the regions of disordered chains, they are confined by the ordered crystallites. The highly ordered crystalline region limits how the water molecules can penetrate into the amorphous region, thus decreasing the degradation rate. Therefore, the rate of water diffusion through the bulk samples plays a key role in the degradation of PGA and PGA-*co*-PLA in the aqueous media. In the following sections, we will discuss several critical morphological factors governing the in vitro degradation process, which can be determined by WAXD and SAXS methods.

Crystallinity and Unit Cell Dimensions. Parts a and b of Figure 4 show the represented WAXD powder profiles extracted from the two-dimensional (2-D) WAXD patterns during in vitro degradation of PGA and PGA-*co*-PLA, respectively. Two strong reflection peaks (110) and (020) and one weak reflection (121) are clearly seen, which are located at 22°, 29°, and 36°, respectively. Another additional reflection (101) superimposes with one of the strong reflections (110) and is discernible as a shoulder reflection peak at 21°. These peaks are assigned on the basis of the orthorhombic unit cell structure of both PGA and PGA-*co*-PLA samples.[12] After the deconvolution of the WAXD profile, the mass degree of crystallinity, ϕ_{mc}, can be obtained. Changes of ϕ_{mc} for the crystalline PGA and PGA-*co*-PLA samples during degradation in PBS are shown in Figure 5. A large increase in ϕ_{mc} for both samples can be seen within the first 2 weeks, then a gradual increase is detected in

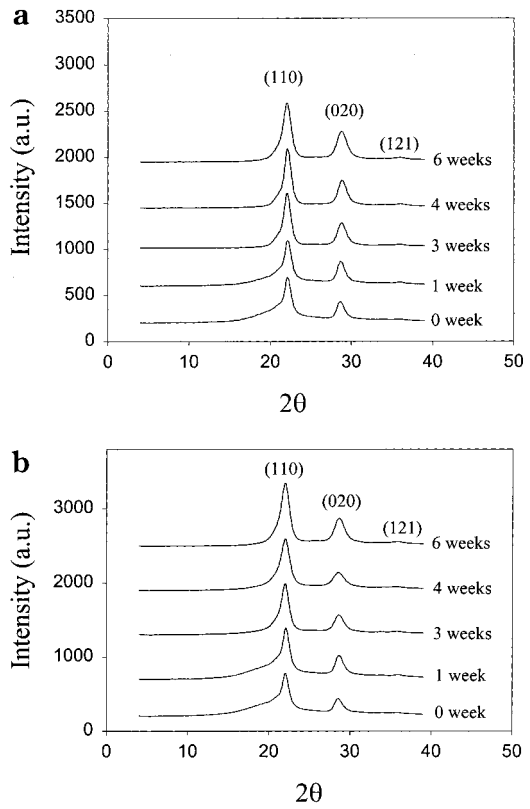

Figure 4. Selected WAXD profiles for the crystalline (a) PGA and (b) PGA-*co*-PLA samples during in vitro degradation.

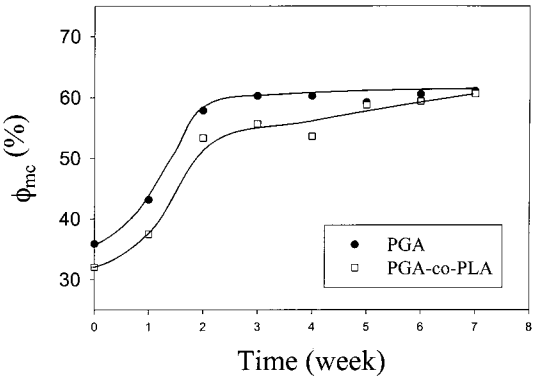

Figure 5. Changes of degree of crystallinity of crystalline PGA and PGA-*co*-PLA samples during in vitro degradation.

PGA-*co*-PLA, and a constant value is found in PGA. Both processes follow an Avrami-like crystallinity increase. We note that the initial PGA-*co*-PLA sample has a lower crystallinity than the initial PGA sample, but the maximum crystallinity at the end of the experiment (7 weeks of degradation) is about the same (60%) for both PGA and PGA-*co*-PLA samples. The increase in crystallinity during hydrolytic degradation has been observed in both PGA and PGA-*co*-PLA samples before.[11,12,17] These observations have been explained by cleavage-induced crystallization as the tie chains in the amorphous regions can degrade into fragments, resulting in a lesser degree of entanglement by the long-chain molecules in the amorphous regions. We will elaborate the cleavage-induced crystallization behavior through the additional SAXS experiment based on the dual lamellar stacks model in the next section.

The positions of the (110), (020), and (121) reflections can be used to determine the dimensions of the crystal unit cell for both PGA and PGA-*co*-PLA samples. The

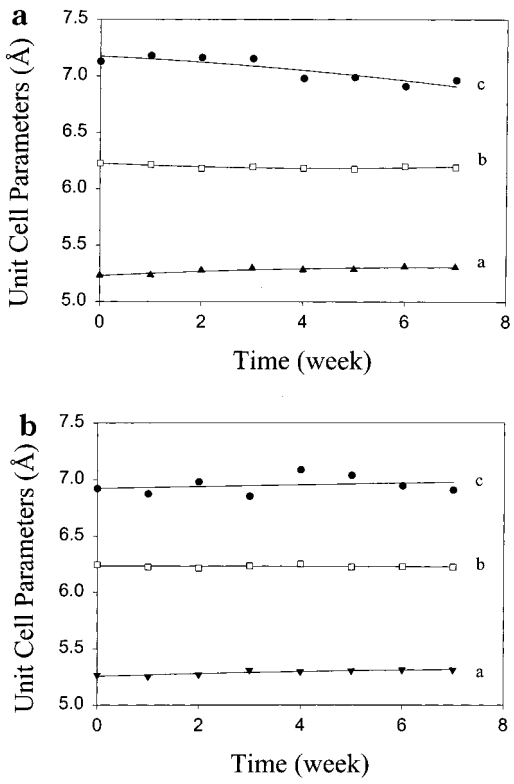

Figure 6. Changes of unit cell parameters of crystalline (a) PGA and (b) PGA-*co*-PLA samples during in vitro degradation. (The symbol ▲ represents the *a* parameter, □ represents the *b* parameter, and ● represents the *c* parameter.)

results are displayed in Figure 6. The unit cell parameters determined here are in reasonable agreement with values reported by Chatani et al. ($a = 5.22$ Å, $b = 6.19$ Å, and $c = 7.02$ Å).[22] The unit cell dimension along the *b* axis shows a slight decrease while that along the *a* axis shows a slight increase (PGA in Figure 6a and PGA-*co*-PLA in Figure 6b) with degradation time, which has been reported before.[17] The values of *a* and *b* are almost the same for PGA and PGA-*co*-PLA. It is, however, interesting to see that the unit cell dimension along the *c* axis shows an opposite change in PGA versus PGA-*co*-PLA samples during degradation. In PGA, the unit cell dimension along the *c* axis decreases (with a larger initial value too), but in PGA-*co*-PLA, the dimension increases with degradation time. Although the effect of degradation on the unit cell dimensions is small, the observed changes reflect the overall increase in crystal perfection, probably accomplished by the removal of constraints on the crystal surfaces. (This is certainly the case of PGA.) This observation is consistent with the scission of the tie chains between the crystal and amorphous phases which alleviates much of the stress on the crystal regions. It is interesting to note that there is no unit cell dimension expansion (in the starting materials) in the copolymer of PGA-*co*-PLA. This suggests that the repeat units of PGA and PLA not only do not cocrystallize, but few PLA moieties are segregated on the PGA crystal surfaces (otherwise the PGA unit cell dimensions will expand), probably due to the low concentration.

Lamellar Morphology Changes. Figure 7a shows the selected SAXS profiles obtained from the crystalline PGA sample during in vitro degradation process. Similar profiles are shown in Figure 7b for the crystalline PGA-*co*-PLA copolymer under the same experimental

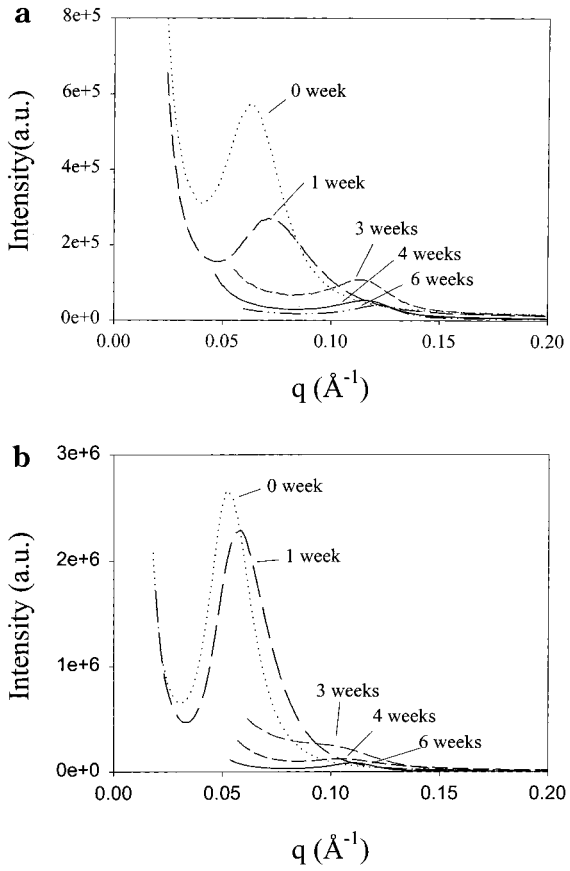

Figure 7. Selected SAXS profiles for crystalline (a) PGA and (b) PGA-*co*-PLA samples during in vitro degradation.

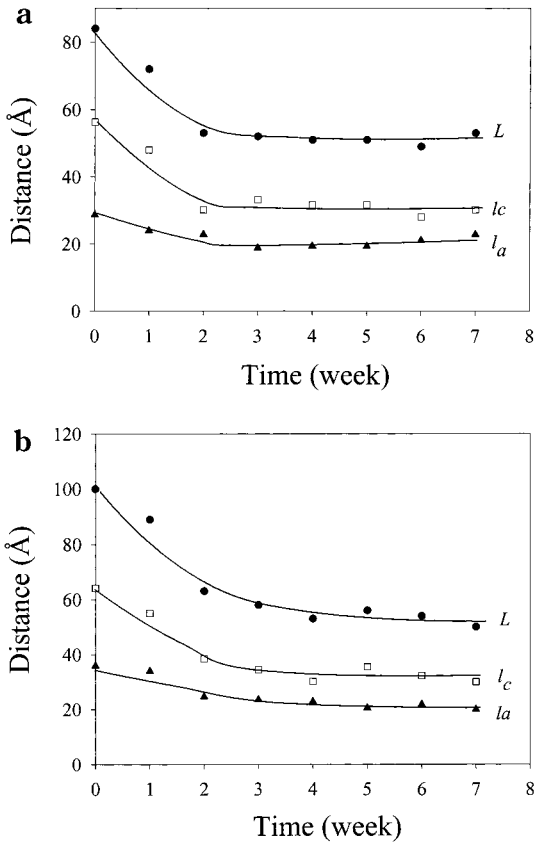

Figure 8. Morphological parameters (L, l_c, and l_a) extracted from SAXS data of (a) PGA and (b) PGA-*co*-PLA samples during in vitro degradation. (The symbol ● represents the long spacing L, ▲ represents the interlamellar amorphous thickness l_a, and □ represents the crystal lamellar thickness l_c.)

conditions. In these figures, it is apparent that the SAXS peak shifts to high value of q (scattering vector defined as $4\pi \sin(\theta)/\lambda$, where 2θ is the scattering angle) with degradation time. The morphology parameters at the lamellar level can be extracted from these SAXS profiles using the method of correlation function.[19] Therefore, several morphological variables including long period L, lamellar thickness l_c, and amorphous layer thickness l_a (assuming that the system follows a two-phase lamellar stacks model) are obtained, and the results are shown in Figure 8. As the correlation function method only yields the values of two average thicknesses in the two-phase lamellar model (l_1 and l_2), we have assigned the larger value l_1 as the lamellar thickness l_c and the lower value l_2 as the amorphous layer thickness l_a. The reason for this assignment can be found in a recent SAXS paper on these biodegradable polymers and will not be elaborated here.[19] In Figure 8 (a and b), the values of L and l_c of both PGA and PGA-*co*-PLA samples are found to decrease rapidly during the first 3 weeks and then remain nearly constant during the subsequent period. The amorphous layer thickness (l_a) between the crystal lamellae for PGA and PGA-*co*-PLA samples also shows a decrease in the first 3 weeks but with a smaller value. It is seen that the values of L, l_c, and l_a in the PGA-*co*-PLA copolymer are higher than that of PGA homopolymer. This can be attributed to the lower degree of supercooling ($T_m - T_c$, where T_c is the crystallization temperature) in PGA-*co*-PLA at the chosen crystallization temperature 110 °C. The decrease in long period, L, during the early stage of hydrolysis degradation has also been reported in PGA or PGA-*co*-PLA samples.[12,17] A lower value of long period is also observed in PGA during degradation as compared with its copolymers in ref 17. The morphological parameters during the degradation of the crystalline PGA and PGA-*co*-PLA samples are summarized in Table 2.

In Table 2, it is interesting to see that the crystal lamellar thickness (l_c) reaches a plateau value around 30 Å in both PGA and PGA-*co*-PLA (90/10) samples after an extensive period of degradation (7 weeks). The corresponding molecular weight in these samples is in the range of 2400 g/mol, which has an average length about 100 Å, which is about 3 times the crystal thickness ($l_c = 30$ Å).

The Degradation Pathways. For the crystalline PGA and PGA-*co*-PLA samples, results show that the degree of crystallinity increases significantly during the initial degradation period, consistent with results reported earlier.[7,11,12,17] For this phenomenon, different explanations have been proposed, which include the cleavage-induced crystallization and the preferential degradation of the amorphous chains. On the basis of this study, as well as previous investigations, we proposed a degradation mechanism as follows. As the bulk crystalline polymers contain alternating crystalline and amorphous regions, some polymer chains will pass through several crystalline and amorphous domains while other chains will return to the same crystallite, but not necessarily in juxtaposition. The crystalline regions contain sequences of highly ordered and preferred conformation chains. The amorphous regions contain chain folds, chain ends, and tie-chain segments in disordered conformations. We believe that degradation will proceed in two different stages: the first stage in the amorphous region and the second stage in the

Table 2. Morphological Parameters of Crystalline PGA and PGA-*co*-PLA (90/10) during in Vitro Degradation

		time (weeks)							
		0	1	2	3	4	5	6	7
PGA	L (Å)	84	72	53	52	51	51	49	53
	l_c (Å)	56	48	30	33	32	32	28	30
	l_a (Å)	28	24	23	19	19	19	21	23
	l_c/L (%)	67.1	66.7	56.9	63.9	62.1	62.1	57.1	56.9
	ϕ_{mc} (%)	35.9	43.2	57.9	60.3	60.3	59.2	60.5	61.1
	ϕ_{vc} (%)	33.1	40.2	54.8	57.3	57.3	56.1	57.5	58.1
	a (Å)	5.24	5.24	5.28	5.30	5.29	5.29	5.31	5.31
	b (Å)	6.23	6.22	6.18	6.20	6.18	6.18	6.20	6.19
	c (Å)	7.13	7.18	7.16	7.16	6.98	6.99	6.91	6.96
PGA-*co*-PLA (90/10)	L (Å)	100	89	63	58	53	56	54	50
	l_c (Å)	64	55	38	34	30	35	32	30
	l_a (Å)	36	34	35	24	23	21	22	20
	l_c/L (%)	64.1	61.2	60.9	59.3	56.9	63.3	59.6	60.0
	ϕ_{mc} (%)	32.0	37.5	53.3	55.7	53.6	58.8	59.4	60.6
	ϕ_{vc} (%)	29.9	35.2	50.9	53.3	51.2	56.4	57.0	58.2
	a (Å)	5.27	5.25	5.27	5.31	5.30	5.31	5.31	5.31
	b (Å)	6.25	6.23	6.22	6.24	6.25	6.23	6.23	6.22
	c (Å)	6.92	6.88	6.98	6.85	7.09	7.04	6.94	6.91

crystalline region. As the diffusion of the water molecules into the amorphous regions is relatively easy, the hydrolytic degradation will begin in the amorphous chains. If the tie chains in the amorphous/crystal interface can be broken by the hydrolysis, the restraints of the long-chain molecules on both amorphous and crystalline regions will be reduced, which leads to higher chain mobility. This facilitates the crystallization process in the amorphous chains[11] and the degradation of the crystalline regions (initiated from the surface). A considerable amount of accessible amorphous material can be crystallized through the scission of amorphous chains with significant increase in mobility, resulting in very high crystallinity, but low molecular weight. Additionally, as the molecular weight of the polymer decreases, amorphous oligomers can diffuse out, leading to further increases in the overall crystallinity level of the remaining polymer material.

With the combined results from GPC, WAXD, and SAXS, we have obtained some new insights into the process of degradation-induced crystallization. This is similar to the dual lamellar stacks model proposed for the thermal crystallization processes of polymers, commonly called primary and secondary crystallization. To begin our discussion, we first examine the WAXD results during degradation of PGA-*co*-PLA amorphous samples (as shown in Figure 9). It is seen from Figure 9a that before degradation only an amorphous scattering halo is present in WAXD. After 1 week of degradation, the strong crystal reflection peaks (110) and (020) begin to appear in WAXD. The corresponding changes of crystallinity are shown in Figure 9b. Crystallinty sharply increases from 0 to 52% within the first 3 weeks of hydrolysis and then plateaus. We believe this is a direct result of cleavage-induced crystallization in the amorphous regions.

From the SAXS data, we believe that the dual lamellar stacks model can best describe the crystal morphology of the PGA and PGA-*co*-PLA (co)polymers. The detailed discussion of this argument has been elaborated elsewhere.[19] The schematic diagram of the degradation process in the lamellar stack model is shown in Figure 10. In this model, the crystalline morphology consists of lamellar stacks in bundles with large amorphous gaps (>100 nm) between them. The lamellar stacks contain alternating crystal lamellar phase (thickness l_c) and amorphous lamellar phase

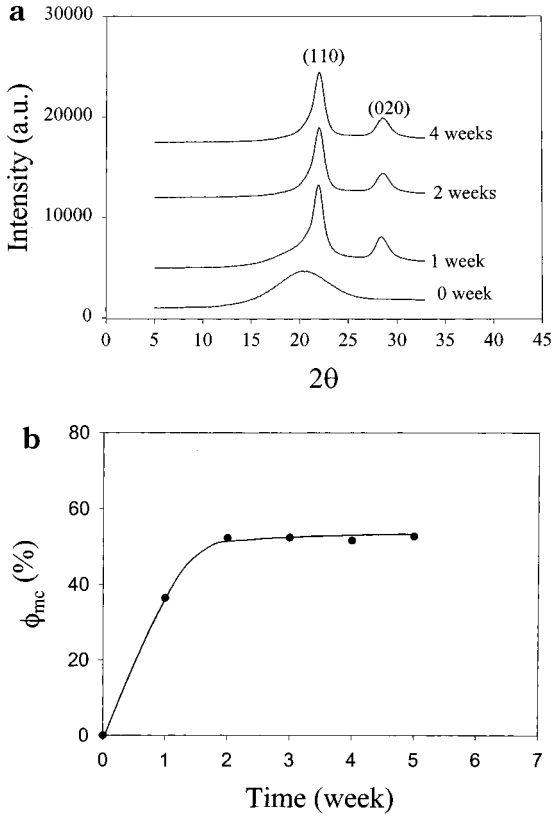

Figure 9. (a) Selected WAXD profiles and (b) degree of crystallinity of PGA-*co*-PLA (90/10) amorphous sample during in vitro degradation.

(thickness l_a). The sum of the values for l_c and l_a is the long period (L), which corresponds to the scattering maximum seen in SAXS. It is know that the secondary crystallization can proceed in this morphology, forming thinner crystallites in the amorphous gaps, and result in dual population of lamellar stacks. This has been seen in many crystalline polymers[18,20] including PGA and PGA-*co*-PLA polymers.[19] From SAXS determination, the values of long period, lamellar thickness, and amorphous layer thickness are statistically averaged.

As the degradation process is initiated by the diffusion of water molecules into the amorphous gaps, causing the scission of polymer chains, this will increase the chain mobility and facilitate the crystallization process in the amorphous gaps that is similar to the secondary

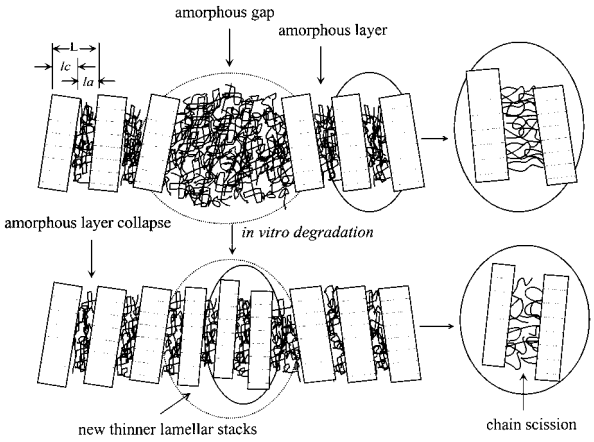

Figure 10. Schematic diagram of in vitro degradation mechanism in the dual lamellar stacks model of semicrystalline samples.

crystallization process from the polymer melt.[24] Due to confined spatial restrictions and lower molecular mass species in the amorphous gaps, the resultant lamellar thickness by cleavage-induced crystallization is thinner, which causes the averaged long period and lamellar thickness to decrease (as seen in Figure 8). In PGA, the values of L and l_c decrease from 84 and 56 Å to 52 and 33 Å, respectively, after 3 weeks of degradation. In PGA-*co*-PLA, the values of L and l_c decrease from 100 and 64 Å to 58 and 34 Å, respectively, during the same period of degradation. The significant drops in L and l_c indicate that there is a large fraction of amorphous gaps in the sample, as also indicated by the relatively low initial crystallinity (ϕ_{mc} = 35.9% for PGA and 32% for PGA-*co*-PLA) in the samples.

It is seen that cleavage-induced crystallization is almost complete after 3 weeks of in vitro degradation. After that, the initial amorphous gaps are probably totally space-filled with thinner crystallites that no further crystallization can occur. This can be confirmed by comparing the linear volume crystallinity (l_c/L) and the bulk volume degree of crystallinity (ϕ_{vc}) (see Table 2) as follows. It should be noted that the densities of the amorphous PGA and PGA-*co*-PLA samples are 1.50 and 1.48 g/cm^3, respectively, and the densities of 100% crystalline PGA and PGA-*co*-PLA samples are 1.70 and 1.63 g/cm^3, respectively.[23] These densities can be used to convert the mass degree of crystallinity (ϕ_{mc} by WAXD) to volume degree of crystallinity (ϕ_{vc}) in Table 2. Beyond 3 weeks, the values of l_c/L and ϕ_{vc} become very close to each other, indicating that the initial amorphous regions are nearly completely crystallized. The similar values between l_c/L and ϕ_{vc} also confirm our initial assignments of l_1 and l_2. The formation of lamellar stacks by cleavage-induced crystallization can be clearly seen by the SAXS study of the amorphous PGA-*co*-PLA sample during degradation (Figure 11). Prior to the degradation, the SAXS profile shows a monotonic decay. After 1 week of degradation, a scattering peak appears, indicating the development of crystal lamellar structure. Further degradation shifts the scattering peak to a larger q value. Figure 11b shows the lamellar variables extracted from the SAXS analysis during the degradation process. It is seen that much thinner lamellar stacks (L = 48−58 Å) are produced in the amorphous samples than the crystalline samples in the same degradation conditions.

In addition to the amorphous gaps between the lamellar stacks, the role of the amorphous layers within

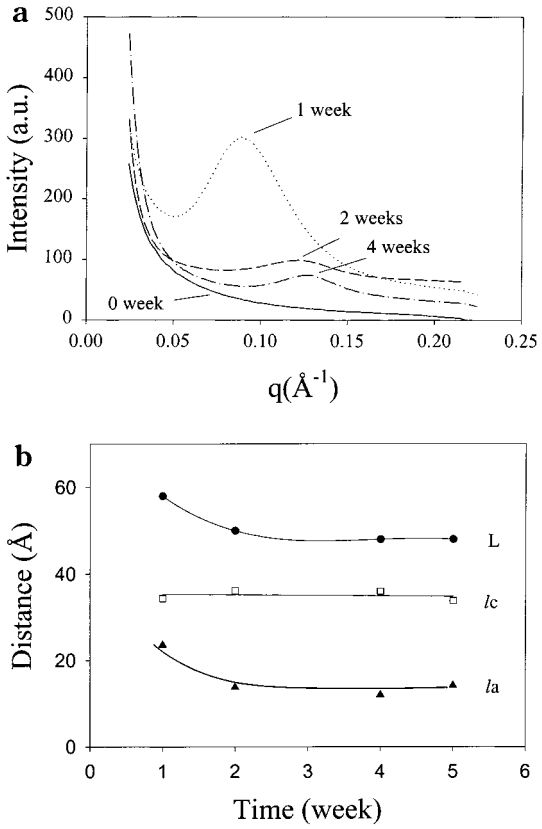

Figure 11. (a) Selected SAXS profiles and (b) lamellar parameters of PGA-*co*-PLA (90/10) amorphous samples during in vitro degradation.

the lamellar stacks must also be important to the degradation process. As these amorphous regions are more confined by the adjacent crystal lamellae (than the amorphous gaps), they probably are not as readily to be degraded as those chains in amorphous gaps. This may be due to the slower diffusion of water molecules into the confined space. However, as these amorphous layers are composed of entanglements, chain ends, and tie chains (in the crystal/amorphous interface), the amorphous chains are still susceptive to hydrolysis. During the early degradation stage (the first 2 weeks) of degradation, the chain scission in the lamellar amorphous layer regions must also occur since the GPC results show significant decreases of number-average molecular weight and polydispersity. It is conceivable that if some coiled amorphous chains are degraded in these regions, the taut tie chains may be relaxed into more energetically favorable conformations, pulling the crystal lamellae closer together and lowering the amorphous layer thickness. This is consistent with the slight decrease of the amorphous layer thickness (l_a) during the first 2 weeks of degradation. The chain cleavage along the interlamellar amorphous layers must be responsible for the sharp decrease of the polydispersity (near the unity) during degradation. What is very interesting is that we find the degraded chain fragments possess an average length about 3 times the crystal lamellar thickness. Perhaps, this result reflects the nature of the chain-folding crystal surface in the polymers that the cleavage can only occur about every other fold due to the statistics or other reasons.

To obtain a better understanding of the cleavage-induced crystallization phenomenon, we have also carried out the weight loss measurements in both amor-

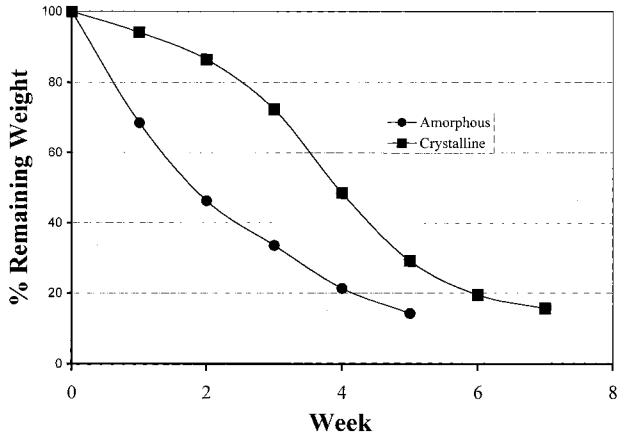

Figure 12. Weight loss profiles of crystalline and amorphous PGA-*co*-PLA (90/10) samples during in vitro degradation.

phous and crystalline PGA-*co*-PLA (90/10) samples, as shown in Figure 12. It is interesting to see that the weight loss of the amorphous sample reaches about 50%, while the loss of the crystalline sample is only about 15%, after 2 weeks of degradation. The large degree of the weight loss in the amorphous sample can be attributed to the many sporadic chain cleavages. The post microstructure developed by cleavage-induced crystallization in a way slightly retards the degradation process, causing the weight loss curve to decay upward. In contrast, the crystalline morphology in the crystalline sample defines the pathways for chain cleavage, which induces a much slower process for the weight loss. We speculate that the weight loss in the crystalline sample is primarily from the amorphous gap regions between the crystal lamellar stacks.

In summary, we believe that there are two possible pathways for the hydrolytic degradation to proceed. (Only one is in conjunction with the event of cleavage-induced crystallization.) The first pathway is through the amorphous gaps between the lamellar stacks, where the scission of the amorphous chains can take place by the diffusion of the water molecules. As the chain scission proceeds, the chain mobility can increase, thus facilitating the secondary crystallization process producing thinner lamellar stacks with lower values of long period (L) and lamellar thickness (l_c). The second pathway is through the interlamellar amorphous layer between the adjacent lamellae within the stacks. As the water molecules can eventually diffuse into this region, the chain scission can lead to the collapse of the lamellar stacks, causing the slight decrease in amorphous layer thickness (l_a).

Conclusion

The changes in structure and morphology in amorphous and crystalline PGA homopolymer and PGA-*co*-PLA (90/10) copolymer during in vitro degradation were investigated by GPC, WAXD, and SAXS. GPC results illustrate that both values of molecular weight and polydispersity decrease significantly within the first 2 weeks of degradation. The rates of degradation for crystalline PGA and PGA-*co*-PLA samples is very similar. WAXD results show an Avrami-like increase in mass degree of crystallinity ϕ_{mc} for both PGA and PGA-*co*-PLA samples during the degradation period. Even as the initial crystalline PGA-*co*-PLA sample has a lower crystallinity than PGA, the final crystallinity during degradation is about 60% for both samples. This behavior is due to cleavage-induced crystallization. The effect of the degradation process on the change in unit cell dimensions is small, but noticeable and anisotropic. Such changes can be explained by crystal perfection. SAXS results show that the long period (L) and lamellar thickness (l_c) of both PGA and PGA-*co*-PLA samples also decrease rapidly during the first 3 weeks of degradation. Interlamellar amorphous layer thickness (l_a) in the crystal stacks also show a slight decrease during the first 3 weeks of degradation for both PGA and PGA-*co*-PLA samples. The combined GPC, WAXD, and SAXS results suggest the hydrolytic degradation proceeds in two possible pathways, both involving chain scission. The first pathway is through the amorphous gaps between the lamellar stacks, where the residual chains may crystallize into new thinner lamellar stacks, leading to large decreases in long period (L) and lamellar thickness (l_c). The second pathway is through the interlamellar amorphous layer between the adjacent lamellae, where chain scission can lead to the rapid decrease of polydispersity.

Acknowledgment. The authors acknowledge the financial support of this work in part by a grant from NSF (DMR 9732653) and in part by Ethicon Inc., A Johnson & Johnson Company.

References and Notes

(1) Zhang, X.; Goosen, F. A.; Wyss, U. P.; Pichor, D. *Rev. Macromol. Chem. Phys.* **1993**, *C33*, 81.
(2) Herrmann, J. B.; Kelly, R. J.; Higgins, G. A. *Arch. Surg.* **1970**, *486*, 100.
(3) Chu, C. C. *The Biomedical Engineering Handbook*; 1995; p 611.
(4) Capperauld, I. *Clin. Mater.* **1989**, *3*, 4.
(5) Gilding, D. K.; Reed, A. M. *Polymer* **1979**, *1459*, 20.
(6) Reed, A. M.; Gilding, D. K. *Polymer* **1981**, *22*, 494.
(7) Gopferich, A. *Biomaterials* **1996**, *103*, 17.
(8) Miller, N. D.; Williams, D. F. *Biomaterials* **1984**, *365*, 5.
(9) Pistner, H.; Bendix, D. R.; Muhling, J.; Reuther, J. F. *J. Biomater.* **1993**, *291*, 14.
(10) Chu, C. C. *J. Biomed. Mater. Res.* **1981**, *15*, 19.
(11) Chu, C. C. *J. Appl. Polym. Sci.* **1981**, *26*, 1727.
(12) Fredericks, R. J.; Melveger, A. J.; Dolegiewitz, L. J. *J. Polym. Sci., Polym. Phys.* **1984**, *57*, 22.
(13) Cohn, D.; Younes, H.; Maron, G. *Polymer* **1987**, *2018*, 28.
(14) Vert, M.; Mauduit, J.; Li, S. *Biomaterials* **1994**, *119*, 15.
(15) Vert, M.; Li, S. M.; Garreau, H. *J. Biomater. Sci., Polym. Ed.* **1994**, *639*, 6.
(16) Vert, M.; Li, S. M.; Garreau, H. *J. Controlled Release* **1991**, *15*, 16.
(17) King, E.; Cameron, R. E. *J. Appl. Polym. Sci.* **1997**, *66*, 1681.
(18) Hsiao, B. S.; Verma, R. K. *J. Synchrotron Radiat.* **1998**, *5*, 23.
(19) Wang, Z. G.; Hsiao, B. S.; Zong, S. X. H.; Zhou, J.; Dormier, E.; Jamiolkowski, D. D. *Polymer*, in press.
(20) Hsiao, B. S.; Sauer, B. B.; Verma, R.; Chu, B.; Harney, P.; Zachmann, H. G.; Seifert, S. *Macromolecules* **1995**, *28*, 6931.
(21) Chu, B.; Harney, P. J.; Li, Y.; Yeh, F.; Hsiao, B. S. *Rev. Sci. Instrum.* **1994**, *65*, 597.
(22) Chantani, Y.; Suehiro, K.; Okita, Y.; Tadokoro, H.; Chujo, K. *Makromol. Chem.* **1968**, *113*, 215.
(23) Chujo, K.; Kobayashi, H.; Suzuki, J.; Tokuhara, S.; Tanabe, M. *Makromol. Chem.* **1967**, *100*, 267.
(24) Verma, R. K.; Hsiao, B. S. *Trends Polym. Sci.* **1996**, *4*, 312.

MA990630P